



High-activity MgO-supported CoMo hydrodesulfurization catalysts prepared by non-aqueous impregnation



Luděk Kaluža*, Daniela Gulková, Zdeněk Vít, Miroslav Zdražil

Institute of Chemical Process Fundamentals of the Academy of Sciences of the Czech Republic, v.v.i., Rozvojová 135, CZ-165 02 Prague 6, Suchdol, Czech Republic

ARTICLE INFO

Article history:

Received 5 May 2014

Received in revised form 3 July 2014

Accepted 7 July 2014

Available online 15 July 2014

Keywords:

CoMo/MgO

Benzothiophene hydrodesulfurization

Non-aqueous impregnation

ABSTRACT

The high surface area MgOs (330 and 500 m² g⁻¹) were studied as supports of Mo and CoMo hydrodesulfurization catalysts. New preparation methods based on impregnation of the supports with methanolic solution of MoO₂- and Co- acetylacetones or dimethylsulfoxide solutions of various Mo and Co compounds with chelating agent nitrilotriacetic acid (NTA) were compared with previously reported method methanol-assisted spreading. The most active CoMo/MgO catalysts exhibited 3.3-fold activities in hydrodesulfurization of benzothiophene as the reference industrial CoMo/Al₂O₃ catalyst.

© 2014 Elsevier B.V. All rights reserved.

1. Introduction

MgO-supported catalysts were mostly studied due to their application in wide range of chemical reaction such as total oxidation [1,2], oxidation of H₂S to sulfur [3,4], oxidative dehydrogenation of hydrocarbons [5,6], dehydrogenation of isopropanol [7,8], CO₂ reforming of methane [9,10], direct internal reforming of methane [11,12], water–gas shift [13,14], methathesis of olefins [15], transesterification of fatty acid esters [16,17], hydrogenation of nitriles to amines [18,19], ammonia synthesis [20,21], synthesis of carbon nanotubes [22,23], and hydrotreating [24–35].

In the field of hydrodesulfurization (HDS), higher basicity of MgO support in comparison to conventionally used γ-Al₂O₃ results in higher dispersion and activity of deposited MoS₂ [24], higher synergy in CoMo phase [25] and higher endurance to coking [26]. These advantages are still insufficiently utilized mainly because of the difficulties with deposition of CoMo active phase onto hydrothermally less stable surface of MgO. Aqueous solutions destroy the texture of MgO during impregnation [27]. Mechanical properties of MgO may also restrict the support to be used in industrial HDS fixed-bed applications [28].

However, we have developed method of the active phase deposition called methanol-assisted spreading that overcomes

deterioration of rather unstable MgO support surface in water during impregnation. Furthermore, we also reported on preparation of the industrially more convenient shaped form of high surface area MgO by re-hydration of commercially available low surface area MgO and calcination [32]. For example, reaction of (NH₄)₆Mo₇O₂₄ [33] or MoO₃ [25,34] with the high surface area MgO in methanol slurry resulted in well-defined saturated Mo monolayer and high activity in HDS of thiophene [34] and benzothiophene [25,33,34]. In the second step, Co was deposited over MoO₃/MgO catalyst from the solution of Co(NO₃)₂ in methanol by impregnation, which resulted in high synergistic effect of Co and about 2-fold increase in activity of benzothiophene HDS than it was observed for conventional γ-Al₂O₃ support [25,34]. The method, however, required rather long reaction times for adsorption of Mo from (NH₄)₆Mo₇O₂₄ [33] or MoO₃ [25,35] slurries.

The aim of the present work is to elucidate on possibility of deposition of molybdenyl- and cobalt- acetylacetones on the high surface area MgO by impregnation from solutions of these compounds in methanol. Furthermore, dimethylsulfoxide solutions of MoO₃ and CoCO₃, (NH₄)₆Mo₇O₂₄ and Co(NO₃)₂, or MoO₂(C₅H₇O₂)₂ and Co(C₅H₇O₂)₂ with chelating agent nitrilotriacetic acid (NTA) were studied for CoMo deposition in one impregnation step.

Selected impregnation methods were studied also over a new commercially available high surface area nano-MgO support. The activity in HDS of 1-benzothiophene was determined to compare the prepared catalyst with industrial reference catalysts supported on conventional γ-Al₂O₃.

* Corresponding author. Tel.: +420 220390270; fax: +420 220920661.

E-mail address: kaluza@icfp.cas.cz (L. Kaluža).

2. Experimental

2.1. MgO

A paste made from 15 g of magnesium carbonate (Sigma-Aldrich, product no. 13138, nominal content of chlorine less than 0.05 wt.%) and 45 ml of distilled water was kneaded in an agate mortar grinder (Fritch, Pulverisette 2) for 15 min. The paste was left standing in a Petri dish on air with occasional mixing with spatula for 30 min until the paste became thick. Then the paste was dried at ambient conditions for 3 days, crushed and sieved to particle size fraction 0.5–2 mm. The particles were washed with distilled water at 70 °C until the water exhibited negative silver nitrate test for the presence of chlorides. The residual chlorides in MgO cause a decrease of specific surface area during calcination [36,37]. The particles were then dried again at ambient conditions for 3 days and they were crushed and sieved to particle size fraction 0.16–0.32 mm. This particle fraction was calcined in air with the flow rate of 9 dm³ min⁻¹ at 390 °C with temperature ramp 15 °C min⁻¹ and dwell time 30 min and stored in gas tight sample bottles. The support was labeled according to its specific surface area 330 m² g⁻¹ MgO-330.

A commercial high surface area nano-MgO (NanoScale Materials Ltd., product no. AC301-0100) was crushed and sieved to particle size fraction 0.16–0.32 mm and calcined as it was described above before use. The support was labeled according to its specific surface area 500 m² g⁻¹ MgO-500.

2.2. Deposition of Mo using methanol solvent

Molybdenum was deposited over the studied supports MgO-330 and MgO-500 by methanol assisted spreading from the slurry MoO₃/methanol and from the solution of molybdenyl acetylacetone in methanol.

MoO₃ (Fluka, product no. 69850) was ground in a planetary mill for 8 h before use. It was mixed with 50 ml of methanol and 5 g of support. Amount 2.14 g of MoO₃ was used to saturate both supports. The mixture was heated under reflux condenser for 48 h. The unreacted slurry of blue-gray MoO₃ was removed from the white-gray catalyst particles by decantation with methanol. The catalysts were dried in a rotary vacuum evaporator at 95 °C for 1 h and labeled as Mo(o)MgO-330 and Mo(o)MgO-500, where the letter "o" refers to oxide. About 2 g of the catalysts were sulfided in hydrogen containing 10% of hydrogen sulfide at 400 °C with temperature ramp 15 °C min⁻¹ and dwell time 1 h. The obtained Mo(o-s)MgO-330 and Mo(o-s)MgO-500 catalysts were packed under nitrogen into gas tight sample bottles and analyzed for Mo content. They contained 16 and 22 wt.% of Mo, respectively.

Another method of Mo deposition was impregnation with the solution of molybdenyl acetylacetone (Alfa Aesar, product no. 44140) in 50 ml of methanol. The amount of molybdenyl acetylacetone corresponded to the actual content of Mo in Mo(o-s)MgO-330 and Mo(o-s)MgO-500. The supports (8 g) were added to the impregnation solution and the mixture was stirred 1 h. The samples were dried in a rotary vacuum evaporator at 95 °C for 1 h and labeled as Mo(a)MgO-330 and Mo(a)MgO-500, where the letter "a" refers to acetylacetone. About 4 g of the catalysts were sulfided, as it was described above, and labeled Mo(a-s)MgO-330 and Mo(a-s)MgO-500. Additionally, the catalyst Mo(a)MgO-330 was calcined in air with the flow rate of 6 dm³ min⁻¹ at 390 °C with temperature ramp 15 °C min⁻¹ and dwell time 30 min. It was labeled as Mo(a-c)MgO-330.

2.3. Promotion with Co using methanol solvent

Impregnation solutions were made by dissolution of cobalt acetylacetone (Fluka, product no. 60801) or cobalt nitrate (Lachema, p.a.) in 20 ml of methanol. The amount of Co corresponded to molar ratio Co/(Co + Mo)=0.3. The mixture of Mo catalyst and the solution was stirred for 1 h and then dried in vacuum rotary evaporator at 95 °C for 1 h. The prepared catalysts were labeled Co(a)Mo(a-c)MgO-330, Co(a)Mo(a)MgO-330, Co(a)Mo(a-s)MgO-330, Co(n)Mo(o)MgO-330, Co(a)Mo(o)MgO-500, Co(a)Mo(o-s)MgO-500, and Co(a)Mo(a-s)MgO-500, where "a" and "n" refer to cobalt acetylacetone and cobalt nitrate, respectively. Part of the sample Co(a)Mo(a)MgO-330 was calcined by the same way as described above and it was named Co(a-c)Mo(a)MgO-330. For the matter of comparison, Co and Mo were deposited simultaneously from the methanolic solution of the acetylacetones using the same loadings, stirring and drying times as described above. The catalyst was named CoMo(a)MgO-330.

2.4. Deposition of CoMo with NTA using DMSO solvent

Mixture of Mo and Co compounds with NTA (Sigma-Aldrich, product no. 72560) was dissolved in dimethylsulfoxide (Schuchardt Munchen, product no. 04196) by gentle stirring and heating at 80 °C under reflux condenser for 8 days. The amount of Mo, Co and NTA was chosen to correspond to 4.4 Mo at. per square nanometer of the support MgO-330, molar ratio Co/Co + Mo=0.3, and NTA/(Co + Mo)=1. The volume of dimethylsulfoxide (DMSO) was 22, 16, and 16 ml for the precursor pairs MoO₃ + CoCO₃ (Sigma-Aldrich, product no. 202193, ground in planetary mill for 8 h), (NH₄)₆Mo₇O₂₄ + Co(NO₃)₂, and MoO₂(C₅H₇O₂)₂ + Co(C₅H₇O₂), respectively. After dissolution of the compounds, 1 g of MgO-330 was added to the impregnation solution. The slurry was stirred at 80 °C for 1 h and then the solvent was gradually evaporated in a vacuum rotary evaporator at 160 °C with temperature ramp 4 °C min⁻¹ and a dwell time 5 h. The samples were labeled CoMo(o,NTA)MgO-330, CoMo(n,NTA) MgO-330, and CoMo(a,NTA)MgO-330.

2.5. Catalyst characterization

The content of Mo and Co in the samples was determined by inductively coupled plasma-atomic absorption spectroscopy (ICP/AAS). X-ray diffraction (XRD) patterns were recorded on a X'Pert instrument (Philips) using Cu K α radiation (40 kV, 40 mA). Specific surface area, S_{N_2} , was determined by N₂ physisorption from the flow of N₂:He (2:8) by Nelsen and Eggertsen method [38] on a Micromeritics FlowSorb III instrument.

Temperature programmed reduction (TPR) was performed in the flow of H₂:Ar (1:19) with a temperature ramp 5 °C min⁻¹ from 40 to 960 °C on a Miromeritics chemisorber AutoChem 2950 HP equipped with a thermal conductivity detector.

The number of unsaturated sites in sulfided Mo and CoMo catalysts was determined by O₂ chemisorption [39]. The sulfided catalysts were flushed by helium (Linde AG, 6.0, Germany) at 400 °C for 1 h and cooled in a mixture of dry ice and ethanol. The amount of chemisorbed O₂ was determined from pulses of O₂ (Linde Gas a.s., Czech Republic) added to the flow of He, which was monitored with a thermal conductivity detector VICI (Valco Instrument Inc., USA) and an HP 3394A integrator (Hewlett Packard, USA).

2.6. HDS of benzothiophene

Benzothiophene (BT) hydrodesulfurization (HDS) was carried out in the gas phase in a fixed-bed tubular-flow microreactor (i.d. 3 mm). The catalysts were presulfided in-situ in a H₂S/H₂ flow

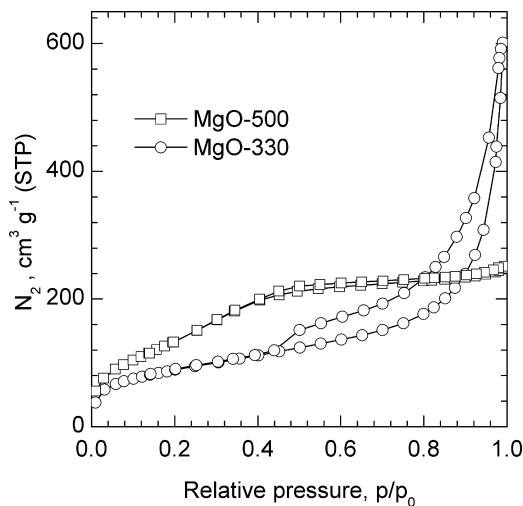


Fig. 1. Nitrogen adsorption–desorption isotherms.

(1/10) at a temperature ramp $10\text{ }^{\circ}\text{C min}^{-1}$ to $400\text{ }^{\circ}\text{C}$ and a dwell time of 1 h. The composition of the starting reaction mixture was kept constant; namely, the mixture contained 16, 200 and 1384 kPa of BT, decane and hydrogen, respectively. The catalyst charge, W , was 0.01 and 0.2 g for CoMo and Mo catalysts, respectively. The reaction was run at $360\text{ }^{\circ}\text{C}$ at three feed rates of BT (F_{BT}): 7.7, 10.3 and 15.5 mmol h^{-1} . The steady state was reached after 30 min after each feed-rate change, with no deactivation of the catalysts observed. The reaction mixture was analyzed with a Hewlett–Packard gas chromatograph (6890 Series) equipped with a capillary column HP-5 (30 m, 0.53 mm, 1.5 μm) and flame ionization detector. The reaction products were dihydrobenzothiophene (DHBT) and ethylbenzene (EB). The total conversion of BT, x_{BT} , and yields of DHBT and EB, y_{DHBT} and y_{EB} , were defined as $x_{\text{BT}} = (1 - n_{\text{BT}}/n_{\text{BT}}^0)$, $y_{\text{DHBT}} = n_{\text{DHBT}}/n_{\text{BT}}^0$, $y_{\text{EB}} = n_{\text{EB}}/n_{\text{BT}}^0$, where n^0 and n were the initial and final numbers of the moles, respectively. The activity of sulfide catalyst was expressed as the empiric rate constant of ethylbenzene formation, k_{EB} , acquired by a non-linear fitting of the dependence y_{EB} on W/F_{BT} using the equation $y_{\text{EB}} = 1 - \exp(-k_{\text{EB}}W/F_{\text{BT}})$. The activities k_{EB} of the prepared catalysts were compared with that of the conventional $\gamma\text{-Al}_2\text{O}_3$ supported Mo (BASF, product no. M8-30) and CoMo (Albemarle, product no. KF756) industrial catalysts.

2.7. Packing density

For the purpose of meaningful comparison with the industrial reference catalysts, the packing density of the prepared and industrial catalysts in the form of grain 0.16–0.32 mm that was used for the activity measurements was determined on an analytical balance in a 2-ml measuring cylinder with inert diameter of 0.8 mm after five-time dabbing off. The packing density, PD, of sulfided catalysts is summarized in Table 1.

3. Results and discussion

3.1. Supports

The adsorption–desorption isotherms of N_2 for both studied MgO supports are shown in Fig. 1. Specific surface area, S_{BET} , was calculated by standard Brunauer–Emmett–Teller (BET) procedure and it was 326 and $504\text{ m}^2\text{ g}^{-1}$ for the support MgO-330 and MgO-500, respectively. Because there were developed knees of the isotherms at partial pressures 0–0.05 over both samples, it was elucidated on the volume of the micropores, V_{Micro} , and specific surface area of the mesopores, S_{M} , by the t-plot method. It was found that

volumes of micropores V_{Micro} were 25 and $52\text{ mm}^3\text{ g}^{-1}$ for MgO-330 and MgO-500, respectively. These V_{Micro} s represented rather formal values of micropore areas of 18 and $37\text{ m}^2\text{ g}^{-1}$, respectively. The value of S_{M} was 280 and $420\text{ m}^2\text{ g}^{-1}$, respectively, and it did not significantly differ from S_{BET} . It was thus concluded that both supports exhibited low volumes of micropores, which is also quite typical for conventional hydrodesulfurization catalysts. For example, we have previously determined V_{Micro} of 25 and $73\text{ mm}^3\text{ g}^{-1}$ for the conventional Mo (BASF) and CoMo (Albemarle) catalysts supported on $\gamma\text{-Al}_2\text{O}_3$ [40], respectively. The S_{BET} s were therefore considered as representative textural parameters and they were used as references for simplified single point surface area, S_{N_2} , determination further in this work.

3.2. Catalysts preparation

The specific surface area S_{N_2} and Co and Mo content in the prepared and sulfided catalysts are summarized in Table 1. It was found that reaction of MoO_3 with the supports MgO-330 and MgO-500 in methanol (samples Mo(o)MgO-330 and Mo(o)MgO-500) resulted in practically the same saturation adsorption density of Mo on the support surface about 4 Mo at. nm^{-2} . This value is slightly higher than $3.4\text{ Mo at. nm}^{-2}$ we determined before for MgO extrudates [35] or Al_2O_3 [41] but still within the range reported in the literature about saturation adsorption monolayer [42–50]. Table 1 also revealed that deposition of Co and Mo onto MgO-330 by methanol-assisted spreading and methanolic impregnation did not significantly influence specific surface areas S_{N_2} . In contrast, S_{N_2} of the catalysts prepared by impregnation of MgO-330 from dimethylsulfoxide solution containing NTA and all catalysts made from MgO-500 were systematically lower than S_{N_2} of original MgO-330 and MgO-500, respectively. Textural instabilities of the high surface area MgO-500 and relative long drying time and high temperature of drying of the NTA containing samples may explain those decreases. Nonetheless, all prepared catalysts exhibited similar S_{N_2} as the reference industrial Mo and CoMo catalysts.

X-ray diffraction measurements did not show Mo-containing crystalline phase. Only broad and low intensity signal of cubic MgO was identified in the sulfided catalysts. These suggested that the deposited species were well dispersed over the support surface or they were in an X-ray amorphous phase.

It was concluded that 1.5-fold higher specific surface area of MgO-500 enabled dispersion of proportionally higher loading of Mo in comparison to MgO-330.

3.3. TPR and chemisorbed O_2

TPR patterns of the catalysts in dried and sulfide form are shown in Figs. 2 and 3, respectively. The consumptions of hydrogen in the first reduction peaks recorded over sulfide catalysts between 30 and $280\text{ }^{\circ}\text{C}$ are summarized in Table 2 along with amount of chemisorbed oxygen.

TPR of dried form of the samples resulted in rather complex patterns (Fig. 2). Negative peaks in hydrogen consumption clearly showed on the presence of organic phase in the samples, which results in methane formation during TPR. A hydrogen consumption thus could not be quantified. Nevertheless, systematic trends were observed for Mo/MgO catalysts. Mo species deposited from the acetylacetone exhibited the first reduction peak at about $550\text{ }^{\circ}\text{C}$ while Mo species deposited from MoO_3 /methanol slurry exhibited the first reduction peak at higher temperature about $600\text{ }^{\circ}\text{C}$. These well correspond with HDS activity (Table 3). Mo/MgO catalysts prepared from the acetylacetone resulted in slightly higher activity than those prepared from MoO_3 /methanol slurry. Mo species in the reference industrial catalyst $\text{Mo/Al}_2\text{O}_3$, however, exhibited the

Table 1
Properties of sulfided catalysts.

Sample	PD (g cm ⁻³)	S_{N_2} (m ² g ⁻¹)	Co (wt.%)	Mo (wt.%)
Catalysts prepared using methanol solvent				
Mo(o)MgO-330	0.34	299	–	16.1
Mo(a)MgO-330	0.29	271	–	15.3
Co(n)Mo(o)MgO-330	0.35	295	3.3	13.3
Co(a)Mo(a)MgO-330	0.30	216	3.4	12.2
Co(a-c)Mo(a)MgO-330	0.33	334	3.6	13.6
Co(a)Mo(a-c)MgO-330	0.33	279	2.6	13.4
Co(a)Mo(a-s)MgO-330	0.29	352	2.0	13.0
CoMo(a)MgO-330	0.31	272	2.6	14.2
CoMo(a-c)MgO-330	0.64	260	2.6	14.1
Mo(o)MgO-500	0.50	362	–	21.6
Mo(a)MgO-500	0.50	324	–	21.3
Co(a)Mo(o)MgO-500	0.54	349	2.1	21.0
Co(a)Mo(o-s)MgO-500	0.66	326	2.8	20.1
Co(a)Mo(a-s)MgO-500	0.35	203	2.9	20.4
Catalysts prepared using DMSO solvent				
CoMo(o,NTA)MgO-330	0.52	195	3.5	15.0
CoMo(a,NTA)MgO-330	0.37	184	3.4	15.4
CoMo(n,NTA)MgO-330	0.47	194	3.7	15.3
Reference catalysts				
Mo-Al ₂ O ₃ (BASF)	0.55	218	–	10.9
CoMo-Al ₂ O ₃ (KF756)	0.65	325	2.8	11.3

Table 2
TPR and O₂ chemisorption over the sulfided catalysts.

Sample	Chemisorbed O ₂ (μmol g ⁻¹)	H ₂ consumption (a.u.)
Catalysts prepared using methanol solvent		
Mo(o)MgO-330	45	0.19
Mo(a)MgO-330	44	0.18
Co(n)Mo(o)MgO-330	65	0.19
Co(a)Mo(a)MgO-330	51	0.21
Co(a-c)Mo(a)MgO-330	59	0.23
Co(a)Mo(a-c)MgO-330	70	0.19
Co(a)Mo(a-s)MgO-330	47	0.20
CoMo(a)MgO-330	50	0.22
CoMo(a-c)MgO-330	48	0.15
Mo(o)MgO-500	46	0.16
Mo(a)MgO-500	23	0.15
Co(a)Mo(o)MgO-500	74	0.18
Co(a)Mo(o-s)MgO-500	57	0.24
Co(a)Mo(a-s)MgO-500	37	0.17
Catalysts prepared using DMSO solvent		
CoMo(o,NTA)MgO-330	55	–
CoMo(a,NTA)MgO-330	65	–
CoMo(n,NTA)MgO-330	51	–
Reference catalysts		
Mo-Al ₂ O ₃ (BASF)	18	0.11
CoMo-Al ₂ O ₃ (KF756)	36	0.15

first reduction peak at about 400 °C despite its relatively low HDS activity. MgO support thus significantly decreased the reducibility of deposited Mo by hydrogen in comparison to Al₂O₃ support.

Within CoMo/MgO catalysts, the catalysts prepared by deposition of cobalt acetylacetone onto sulfided form of Mo/MgO (samples Co(a)Mo(a-s)MgO-330, Co(a)Mo(o-s)MgO-500, Co(a)Mo(o-s)MgO-500) consumed hydrogen at significantly lower temperatures between 150 and 450 °C than the other samples. TPR patterns were therefore mostly governed by the presence of sulfided molybdenum. The TPR pattern of NTA containing samples was the least resolved.

In contrast, TPR of sulfided form of the samples resulted in qualitatively better resolved patterns (Fig. 3) than TPR of dried form. Due to complete pre-sulfidation, the negative peaks of methane were not observed. Studied sulfided catalysts exhibited typical first reduction peak in temperature range about 120–280 °C. The Mo/MgO-500 catalysts with higher loadings of Mo exhibited the

Table 3
Activities of the prepared and reference sulfide catalysts in HDS of benzothiophene (k_{EB}) and promotional effect of Co (PE).

Catalysts	k_{EB} (mmol _{EB} g ⁻¹ h ⁻¹)	PE ($k_{EB}(\text{CoMo})/k_{EB}(\text{Mo})$)
Catalysts prepared using methanol solvent		
Mo(o)MgO-330	36	–
Mo(a)MgO-330	42	–
Co(n)Mo(o)MgO-330	1653	46
Co(a)Mo(a)MgO-330	932	22
Co(a-c)Mo(a)MgO-330	1624	39
Co(a)Mo(a-c)MgO-330	1139	27
Co(a)Mo(a-s)MgO-330	1545	37
CoMo(a)MgO-330	963	23
CoMo(a-c)MgO-330	1091	26
Mo(o)MgO-500	59	–
Mo(a)MgO-500	66	–
Co(a)Mo(o)MgO-500	765	13
Co(a)Mo(o-s)MgO-500	1256	21
Co(a)Mo(a-s)MgO-500	1232	19
Catalysts prepared using DMSO solvent		
CoMo(o,NTA)MgO-330	1386	–
CoMo(a,NTA)MgO-330	1751	–
CoMo(n,NTA)MgO-330	1754	–
Reference catalysts		
Mo-Al ₂ O ₃ (BASF)	32	–
CoMo-Al ₂ O ₃ (KF756)	462	–

first reduction peak at lower temperatures than Mo/MgO-330 catalysts with lower loadings of Mo. Similar correlation was previously reported for MoS₂/Al₂O₃ catalysts activated in hydrogen sulfide/hydrogen mixture [51,52]. It was concluded that TPR of sulfided Mo deposited over MgO was mostly influenced by the support type and loadings of Mo than by the type of Mo precursors or method of Mo deposition. High surface area of MgO-500 dispersed high amount of Mo, which results in lower reduction temperature and higher activity in HDS. Nevertheless, we did not observe correlation between amount of consumed hydrogen in the first reduction peak and activity in HDS.

All sulfided CoMo catalysts exhibited the first reduction peak slightly shifted to the lower temperatures than it was observed for Mo catalysts. However, no correlation was found among reduction temperature, hydrogen consumption, chemisorbed oxygen or activity in HDS reaction for CoMo/MgO catalysts.

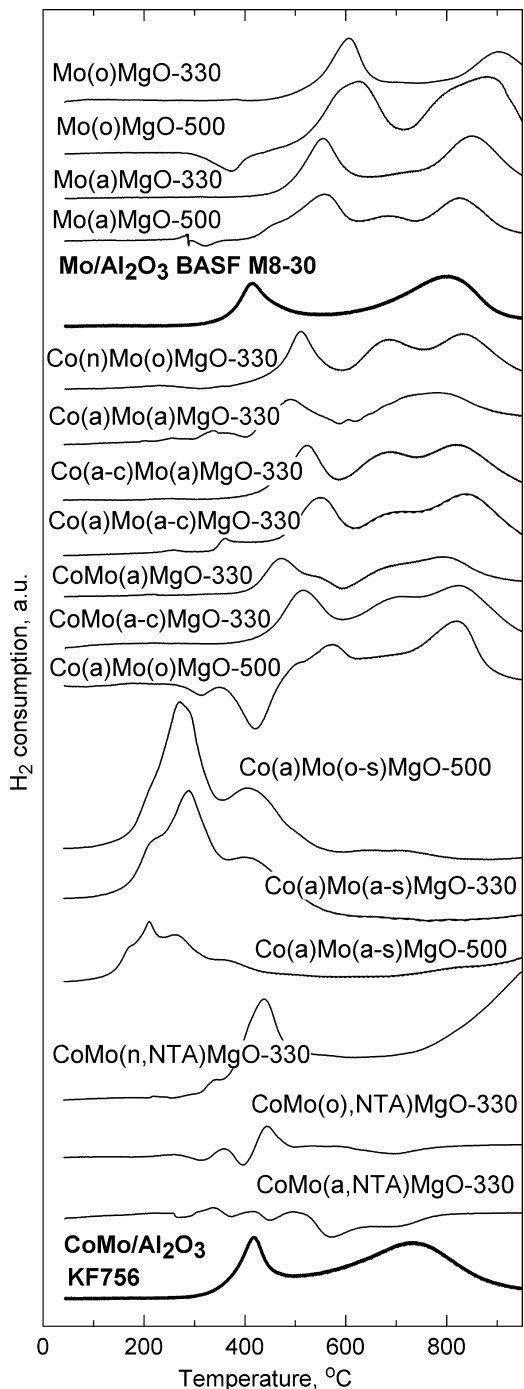


Fig. 2. Temperature programmed reduction of dried catalysts.

3.4. HDS of 1-benzothiophene

The 1-benzothiophene was converted to dihydrobenzothiophene (DHBT) by C=C bond hydrogenation (HYD) and ethylbenzene (EB) and hydrogen sulfide by C–S bond hydrogenolysis (HYG). Further portion of EB and H₂S was formed by HYG of dihydrobenzothiophene. An example, how the integral HDS activity index k_{EB} was quantified is provided in Fig. 4 and k_{EBS} are summarized in Table 3. The selectivity HYD/HYG is expressed as a dependence of yield of DHBT (y_{DHBT}) on total conversion of BT (x_{BT}) in Fig. 5.

It was found that about 1.5 higher surface area of MgO-500 was able to disperse about 1.3–1.4 higher amount of Mo (Table 1), which resulted in only 1.2 times higher surface area of sulfide

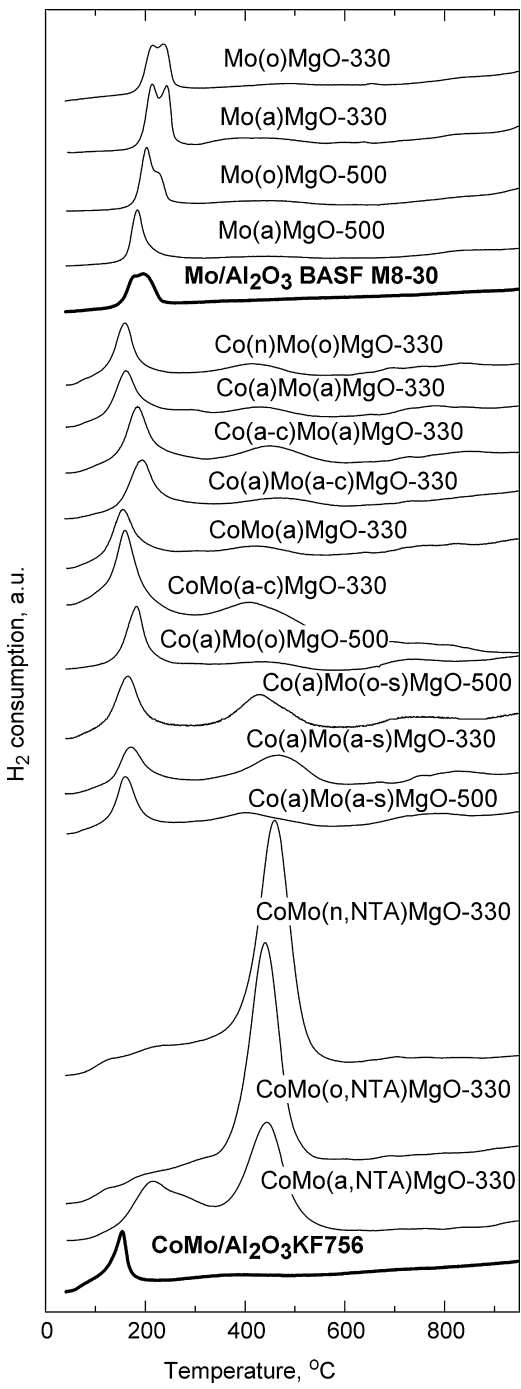


Fig. 3. Temperature programmed reduction of sulfided catalysts.

Mo catalysts but in 1.6 times higher activity in HDS, in comparison to MgO-330 (Table 3). Intrinsic activity of Mo, the activity normalized per gram of Mo, was therefore calculated from k_{EB} to compare all Mo catalysts. The intrinsic activity exhibited values of 224, 275, 273, and 310 mmol_{EB} g(Mo)⁻¹ h⁻¹ over Mo(o)MgO-330, Mo(a)MgO-330, Mo(o)MgO-500, and Mo(a)MgO-500 catalyst, respectively, which were similar and approximately the same as the value of 294 mmol_{EB} g(Mo)⁻¹ h⁻¹ for the reference industrial Mo/Al₂O₃ catalyst. Selectivity HYD/HYG in Fig. 5 also exhibited the same behavior over all studied Mo catalysts. These are in agreement with a monolayer type of Mo deposition over MgO and Al₂O₃ supports. Nonetheless, slightly better quality of Mo deposition and HDS activity (Table 3) was achieved by the deposition of

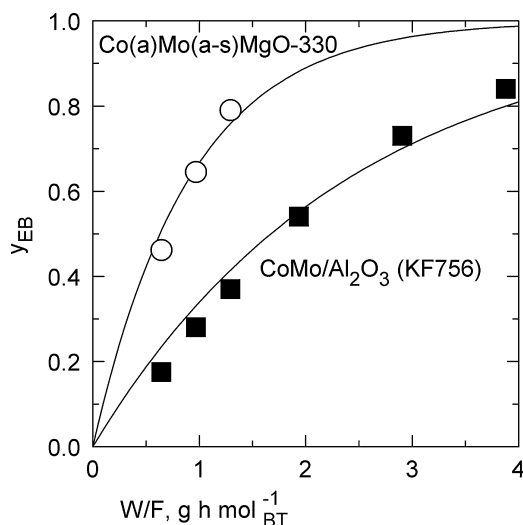


Fig. 4. An example of the activity index, k_{EB} , fitting (solid lines): open circles – Co(a)Mo(a-s)MgO-330 catalyst; filled squares – industrial Al_2O_3 supported CoMo catalyst.

molybdenyl acetylacetone from methanolic solution than by deposition of molybdenum trioxide from methanolic slurry onto both MgO studied. Oxygen uptake or hydrogen consumption for the sulfide catalyst (Table 2) and selectivity HYD/HYG (Fig. 5), however, did not confirm this rather delicate trend.

Preparation of bimetallic CoMo catalysts from acetylacetones and MgO -330 was varied to elucidate on resultant activities and promotional effects of Co (Table 3). First, impregnation without the use of chelating agent NTA is discussed. It was found that co-impregnation of MgO -330 with a solution of molybdenyl and cobalt acetylacetones in methanol (CoMo(a)MgO-330) led to relatively low activity within the studied series. Calcination of this sample did not significantly improve the activity. The promotional effects of Co (PE) were expressed as a ratio of k_{EB} of CoMo catalyst and k_{EB} of Mo counterpart in Table 3. The PEs in CoMo(a)MgO-330 and CoMo(a-c)MgO-330 were also low within the series.

Similar and low activities and PEs were observed for the subsequent impregnation (molybdenyl acetylacetone first and cobalt acetylacetone second) of MgO -330 independently whether the firstly deposited molybdenum species were calcined (sample Co(a)Mo(a-c)MgO-330) or not (sample Co(a)Mo(a)MgO-330). However, calcination of the sample Co(a)Mo(a)MgO-330 significantly (about 1.7 times) improved the activity and promotional effect (Co(a-c)Mo(a)MgO-330).

Similar and high activities and promotional effects were achieved after deposition of cobalt acetylacetone onto pre-sulfidized Mo/MgO catalyst (Co(a)Mo(a-s)MgO-330) and for a catalysts prepared for comparison (Co(n)Mo(o)MgO-330), wherein cobalt was deposited from solution of cobalt nitrate in methanol onto MoO_3/MgO precursor prepared by methanol-assisted spreading of MoO_3 [27,35].

The three most active CoMo/MgO-330 catalysts exhibited at least 3.3-fold higher activities than the reference industrial CoMo catalysts supported on $\gamma\text{-Al}_2\text{O}_3$. In contrast, selectivity HYG/HYD was practical the same over all studied CoMo catalysts (Fig. 5).

Secondly, the use of chelating agent NTA for the co-impregnation of MgO -330 is discussed. It was found that dimethylsulfoxide dissolved molybdenyl and cobalt acetylacetone with NTA in 2 h and cobalt nitrate and ammonium heptamolybdate with NTA in 1 day. Both solutions led to deposited CoMo phase highly active in hydrodesulfurization. The sample

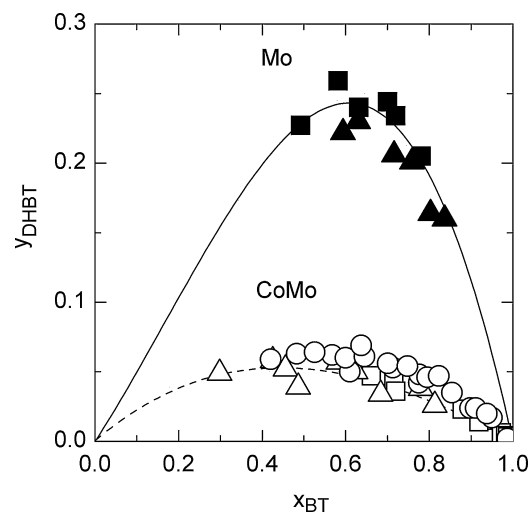


Fig. 5. Selectivity to dihydrobenzothiophene (DHBT) during 1-benzothiophene (BT) HDS: solid line – $\text{Mo}/\text{Al}_2\text{O}_3$ (BASF); dash line – $\text{CoMo}/\text{Al}_2\text{O}_3$ (KF756); solid squares – Mo catalysts over MgO -330; solid triangles – Mo catalysts over MgO -500; open circles – CoMo catalysts (prepared without NTA) over MgO -330; open squares – CoMo catalysts prepared with NTA over MgO -330; open triangles – CoMo catalysts (prepared without NTA) over MgO -500.

CoMo(a,NTA) prepared from the acetylacetones was about 1.8 more active than sample CoMo(a)MgO-330 prepared from the same precursors but without NTA. However, CoMo(n,NTA) prepared from cobalt nitrate and ammonium heptamolybdate resulted in the same activity as CoMo(a,NTA). It was concluded that chelating properties of NTA were the factor governing the resultant activity and not the precursor type.

Nonetheless, the chelating agent did not dissolve entire portion of CoCO_3 and MoO_3 in dimethylsulfoxide despite higher dissolution time and solvent volume, which resulted in rather low activity of the sample CoMo(o,NTA). The catalyst exhibited only about 80% activity of the catalysts samples CoMo(a,NTA) and CoMo(n,NTA), which quite well corresponds with the undissolved amount of the precursors.

To compare co-impregnation method with the use of NTA and subsequent impregnation techniques, the NTA-assisted spreading of the acetylacetones resulted only in 12% increase, which is close to the experimental error of activity tests. The co-impregnation method thus represents relatively simple and straightforward method of deposition of CoMo phase onto hydrothermally low stable MgO . Nevertheless, the need of higher temperature and time during drying in rotary vacuum evaporator does not favor it. The MgO -500 was therefore impregnated subsequently with sulfidation of Mo prior to deposition of cobalt acetylacetone. MgO -500 supported CoMo catalysts did not overwhelm the activity of MgO -330 supported counterparts (Table 3). This highlighted the fact that deposition of Co as an activity promoter represents the most sensitive part of preparation of MgO supported catalysts. Particularly, the high surface area MgO -500 suffered from textural instability despite avoiding water during preparation.

The activities k_{EB} of the prepared CoMo catalysts varied up to 1.9-fold and clearly corresponded with varying preparation parameters in specific cases as it was discussed above. However, the selectivity HYG/HYD in Fig. 4 did not exhibit practically any changes. The MgO supported CoMo catalysts were as selective to dihydrobenzothiophene as the reference industrial CoMo catalysts supported on $\gamma\text{-Al}_2\text{O}_3$. The selectivity results qualitatively corresponded with the results of oxygen chemisorption and TPR. None of these methods reflected on changes in preparation parameters and the HDS activity test remained the most sensitive one.

4. Conclusions

It has been shown that MgO with surface area $S_{\text{BET}} = 500 \text{ m}^2 \text{ g}^{-1}$ was able to disperse higher loading of Mo in comparison with MgO of $S_{\text{BET}} = 330 \text{ m}^2 \text{ g}^{-1}$, which resulted in correspondingly higher activity in HDS of benzothiophene. Impregnation of the supports with methanolic solution of molybdenyl acetylacetone reduced mainly the operation time in comparison to previously reported rather delicate method called methanol-assisted spreading of MoO_3 while keeping the same HDS activity and HYD/HYG selectivity. Deposition of Co, however, showed on textural instability of the MgO support with original $S_{\text{BET}} = 500 \text{ m}^2 \text{ g}^{-1}$. The MgO with $S_{\text{BET}} = 330 \text{ m}^2 \text{ g}^{-1}$ was the support yielding the highest activity of CoMo in HDS. Apart from previously reported deposition of cobalt nitrate from methanolic solution onto MoO_3/MgO catalysts, the most active catalysts were prepared by (i) deposition of cobalt acetylacetone from methanolic solution onto dried form of MgO supported molybdenyl acetylacetone followed by calcination, or (ii) deposition cobalt acetylacetone from methanolic solution onto pre-sulfided Mo/MgO catalysts followed by sulfidation, or (iii) co-impregnation of the MgO with solution made by dissolution of cobalt acetylacetone, molybdenyl acetylacetone and chelating agent nitrilotriacetic acid (molar ratio NTA/(Co + Mo) = 1) in dimethylsulfoxide. The CoMo/MgO catalysts exhibited at least 3.3-fold activities but the same selectivity C=C hydrogenation/C–S hydrogenolysis as the reference industrial CoMo/Al₂O₃ catalyst.

Acknowledgment

The financial support of the Grant Agency of the Czech Republic (Grant no. P106/11/0902) is gratefully acknowledged.

References

- [1] K. Blick, T.D. Mitrelas, J.S.J. Hargreaves, J.G. Hutchings, R.W. Joyner, C.J. Kiely, F.E. Wagner, *Catal. Lett.* 50 (1998) 211–218.
- [2] K. Asakura, H. Nagahiro, N. Ichikuni, Y. Iwasawa, *Appl. Catal. A Gen.* 188 (1999) 313–324.
- [3] E.K. Lee, K.D. Jung, O.S. Joo, Y.G. Shul, *Appl. Catal. A Gen.* 268 (2004) 83–88.
- [4] E.K. Lee, K.D. Jung, O.S. Joo, Y.G. Shul, *Bull. Korean. Chem. Soc.* 26 (2005) 281–284.
- [5] C. Pak, A.T. Bell, T.D. Tilley, *J. Catal.* 206 (2002) 49–59.
- [6] V.V. Chesnokov, A.F. Bedillo, D.S. Heroux, I.V. Mishakov, K.J. Klabunde, *J. Catal.* 218 (2003) 438–446.
- [7] A. Aboukais, R. Bechara, C.F. Aïssi, J.P. Bonnelle, A. Oujour, M. Loukah, G. Coudurier, J.C. Vedrine, *J. Chem. Soc., Faraday Trans.* 89 (1993) 2545–2549.
- [8] S.A. El-Molla, G.A. El-Shobaky, N.H. Amin, M.N. Hammed, S.N. Sultan, *J. Mex. Chem. Soc.* 57 (2013) 36–42.
- [9] Y.H. Wang, H. Wang, Y. Li, Q.M. Zhu, B.Q. Xu, *Top. Catal.* 32 (2005) 109–116.
- [10] R. Zanganeh, M. Rezaei, A. Zamaniyan, *Int. J. Hydrogen Energ.* 38 (2013) 3012–3018.
- [11] R.J. Berger, E.B.M. Doesburg, J.G. van Ommeren, J.R.H. Ross, *Appl. Catal. A Gen.* 143 (1996) 343–365.
- [12] J.S. Choi, J.S. Yun, H.H. Kwon, T.H. Lim, S.A. Hong, H.I. Lee, *J. Power Sources* 145 (2005) 652–658.
- [13] H. Yahiro, K. Murawaki, K. Saiki, T. Yamamoto, H. Yamaura, *Catal. Today* 126 (2007) 436–440.
- [14] H.S. Roh, D.W. Jeong, K.S. Kim, I.H. Eum, K.Y. Koo, W.L. Yoon, *Catal. Lett.* 141 (2011) 95–99.
- [15] S. Hasegawa, T. Tanaka, M. Kudo, H. Mamada, H. Hattori, S. Yoshida, *Catal. Lett.* 12 (1992) 255–266.
- [16] C. Xu, D.I. Enache, R. Lloyd, D.W. Knight, J.K. Bartley, G.J. Hutchings, *Catal. Lett.* 138 (2010) 1–7.
- [17] N. Kaur, A. Ali, *Energ. Source A* 35 (2013) 184–192.
- [18] H. Chen, M. Xue, J. Shen, *Catal. Lett.* 135 (2010) 246–255.
- [19] R.K. Marella, K.S. Koppadi, Y. Jyothi, K.S.R. Rao, D.R. Burri, *New J. Chem.* 37 (2013) 3229–3235.
- [20] B.C. McClain, R.J. Davis, *J. Catal.* 210 (2002) 387–396.
- [21] M. Saito, M. Itoh, J. Iwamoto, C.Y. Li, K. Machida, *Catal. Lett.* 106 (2006) 107–110.
- [22] H. Patel, L.M. Manocha, S. Manocha, *Nanosci. Nanotechnol. Asia* 2 (2012) 66–75.
- [23] W.M. Yeoh, K.Y. Lee, S.P. Chai, K.T. Lee, A.R. Mohamed, *J. Phys. Chem. Solids* 74 (2013) 1553–1559.
- [24] F. Cesano, S. Bertaione, A. Piovano, G. Agostini, M.M. Rahman, E. Groppo, F. Bonino, D. Scarano, C. Lamberti, S. Bordiga, L. Montanari, L. Bonoldi, R. Millini, A. Zecchina, *Catal. Sci. Technol.* 1 (2011) 123–136.
- [25] L. Kaluža, D. Gulková, Z. Vít, M. Zdražil, *Appl. Catal. A Gen.* 324 (2007) 30–35.
- [26] C.C. Xu, H. Su, M. Ghosh, *Energ. Fuel* 23 (2009) 3645–3651.
- [27] T. Klicpera, M. Zdražil, *J. Catal.* 206 (2002) 314–320.
- [28] H. Toulhoat, P. Raybaud, *Catalysis by Transition Metal Sulphides*, Editions Technip, Paris, 2013.
- [29] D. Solis, T. Klimova, J. Ramírez, T. Cortez, *Catal. Today* 98 (2004) 99–108.
- [30] F. Trejo, M.S. Rana, J. Ancheyta, *Catal. Today* 130 (2008) 327–336.
- [31] L. Wu, D. Jiao, L. Chen, J.A. Wang, F. Cao, *Adv. Mat. Res.* 132 (2010) 45–54.
- [32] D. Gulková, O. Šolcová, M. Zdražil, *Micropor. Mesopor. Mater.* 76 (2004) 137–149.
- [33] T. Klicpera, M. Zdražil, *Catal. Lett.* 58 (1999) 47–51.
- [34] J. Cinibulk, P.J. Kooyman, Z. Vít, M. Zdražil, *Catal. Lett.* 89 (2003) 147–152.
- [35] D. Gulková, L. Kaluža, Z. Vít, M. Zdražil, *Catal. Commun.* 7 (2006) 276–280.
- [36] G. Leofanti, M. Solari, G.R. Tauszik, F. Garbassi, S. Galvagno, J. Schwank, *Appl. Catal. A* 3 (1982) 131–139.
- [37] T.E. Holt, A.D. Logan, S. Chakraborti, A.K. Datye, *Appl. Catal.* 34 (1987) 199–213.
- [38] F.M. Nelsen, F.T. Eggertsen, *Anal. Chem.* 30 (1958) 1387–1390.
- [39] V. Schwartz, V.T. da Silva, S.T. Oyama, *J. Mol. Catal. A* 163 (2000) 251–268.
- [40] L. Kaluža, D. Gulková, O. Šolcová, N. Žilková, J. Čejka, *Appl. Catal. A Gen.* 351 (2008) 93–101.
- [41] L. Kaluža, Z. Vít, M. Zdražil, *Appl. Catal. A Gen.* 282 (2005) 247–253.
- [42] J. Vakros, K. Bourikas, C. Kordulis, A. Lycourghiotis, *J. Phys. Chem. B* 107 (2003) 1804–18013.
- [43] Y. Okamoto, Y. Arima, K. Nakai, S. Umeno, N. Katada, H. Yoshida, T. Tanaka, M. Yamada, Y. Akai, K. Segawa, A. Nishijima, H. Matsumoto, M. Niwa, T. Uchijima, *Appl. Catal. A Gen.* 170 (1998) 315–328.
- [44] Y. Okamoto, T. Imanaka, *J. Phys. Chem.* 92 (1998) 7102–7112.
- [45] A.L. Diaz, M.E. Bussell, *J. Phys. Chem.* 97 (1993) 470–477.
- [46] D.S. Zingg, L.E. Makovsky, R.E. Tischer, F.R. Brown, D.H. Hercules, *J. Phys. Chem.* 84 (1980) 2898–2906.
- [47] J.A.R. van Veen, P.A.J.M. Hendriks, E.J.G.M. Romers, R.R. Andréa, *J. Phys. Chem.* 94 (1990) 5275–5282.
- [48] P. Dufresne, E. Payen, J. Grimblot, J.P. Bonnelle, *J. Phys. Chem.* 85 (1981) 2344–2351.
- [49] M. Del Arco, S.R.G. Carrazán, V. Rives, F.J. GilLlambíaz, P. Malet, *J. Catal.* 141 (1993) 48–57.
- [50] Y. Xie, Y. Tang, *Adv. Catal.* 37 (1990) 1–43.
- [51] J.J. Lee, H. Kim, S.H. Moon, *Appl. Catal. B Environ.* 41 (2003) 171–180.
- [52] N. Dinter, M. Rusanen, P. Raybaud, S. Kasztelan, P. Da Silva, H. Toulhoat, *J. Catal.* 267 (2009) 67–77.